Mechanical instabilities in epithelial monolayers: viscoelasticity, line tension, and wetting-driven fingering

Ivana Pajic-Lijakovic[1,2], Milan Milivojevic[1], and Peter V.E. McClintock[2]

[1]University of Belgrade, Faculty of Technology and Metallurgy, Department of Chemical Engineering, Belgrade, Serbia

[2]Department of Physics, Lancaster University, Lancaster LA1 4YB,UK

Correspondence to: Ivana Pajic-Lijakovic, iva@tmf.bg.ac.rs

Peter V.E. McClintock, p.v.e.mcclintock@lancaster.ac.uk

Abstract

Epithelial fingering emerges when the free edge of a collectively migrating monolayer becomes mechanically unstable. Inhomogeneous line tension and spatial differences in adhesion energy relative to cell–cell cohesion guide cells toward mechanically favorable regions at finger tips. This edge-directed migration locally disrupts adherens junctions, promotes leader cell formation, and amplifies protrusive instabilities. Because fingering breaks edge continuity, it perturbs coordinated migration, weakens mechanical coherence, and compromises epithelial integrity during wound closure, morphogenesis, and barrier maintenance. Preventing fingering is therefore essential for preserving directional migration and tissue cohesion.

Monolayer viscoelasticity critically regulates this behaviour. Time-dependent redistribution of residual stresses controls energy storage and dissipation and modulates effective edge line tension. Spatial variations in cell packing density generate isotropic or anisotropic migration patterns that shape in-plane stress gradients and trigger local wetting or de-wetting. Formation of a continuous supracellular actin cable increases line tension and stabilizes the edge, thereby suppressing fingering. Together, these mechanisms provide a theoretical framework linking spatial heterogeneity, viscoelastic stress redistribution, and edge mechanics to the emergence and control of epithelial fingering.

Keywords:viscoelasticity, line tension, epithelial wetting and de-wetting, collective cell migration, Marangoni effect

1.Introduction

Directional collective cell migration is a fundamental process that underlies numerous biological phenomena, including tissue morphogenesis, wound healing, and coordinated tissue remodeling[1,2]. Successful migration requires that cells maintain alignment of motion, balanced mechanical stress distribution, and cohesive interactions across the monolayer[3,4]. The emergence of epithelial fingering, can compromise this coordination by creating local regions of differential stress and adhesion, disrupting coherent, directional migration along the monolayer edge and potentially destabilizing tissue integrity[5-7]. Understanding the mechanisms that regulate edge stability is essential, as the directional migration of the monolayer plays a significant role in tissue spreading and repair.

Epithelial fingering refers to the spontaneous formation of finger-like extensions at the free edge of a migrating epithelial monolayer. The phenomenon arises in monolayers that are highly mobile, weakly cohesive, and capable of forming leader cells. Examples include MDCK II (Madin–Darby Canine KidneyII) cells, MCF10A (Human breast epithelial) cells, HaCaT (human keratinocytes) and others[8-10]. An inhomogeneous distribution of mechanical stress, line tension, cell tractions and variations in the strength of cell–cell and cell–matrix adhesion contacts along the edge stimulate formation of leader cells and on that basis epithelial fingering[8,10]. Leader cells differ from other epithelial cells in that they become larger, exhibit pronounced front–rear polarization, form strong cell–matrix adhesions with increased traction forces, and locally weaken cell–cell junctions, enabling protrusive migration at mechanically unstable regions of the epithelial edge[4,8].

Similar fingering phenomena are observed in soft-matter systems, such as thin elastic or viscoelastic sheets on substrates, where protrusions or wrinkles arise due to the competition between elastic energy, adhesion, and boundary constraints. Yu and Jiang[11] highlighted that the interplay between the adhesion energy (between the elastic sheet and the substrate matrix), and the storage elastic energy contained within the sheet, affects the fingering patterns of the sheet. The fingering of a sheet depends on the viscoelastic and surface tension forces, the elastic properties of the matrix, and the thickness of the sheet[12]. In these systems, instabilities are typically passive, reflecting the cohesion properties of sheets and sheet-matrix adhesion properties and their viscoelasticity. In contrast, epithelial monolayers actively control: (i)the cohesive and adhesive properties by remodeling cell-cell and cell-matrix adhesion contacts, (ii)the residual stress accumulation caused by collective cell migration, and (iii)the line tension along the edge. The line tension indicates the elastic and contractile energy stored per unit edge, depending on the viscoelastic nature of border cells, the strength of cell-cell adhesion connections, and the viscoelasticity of the supracellular actin cable[13], if it exists. The latter is a continuous, belt-like actomyosin structure formed by the coordinated alignment and coupling of actin filaments and myosin II motors across multiple neighbouring cells[14,15]. The actin cable arises from the collective organization of the intracellular actomyosin cytoskeleton in a sequence of adjacent cells. It behaves as a contractile structure on a supracellular scale, mechanically integrating cells along an epithelial boundary and induces an increase in the line tension. This makes active epithelial fingering distinct, as compared to

fingering of soft matter systems as it couples the active response of epithelial collectives in ways that do not occur in passive gels or sheets.

A significant aspect that has often been overlooked in earlier research on epithelial fingering is the viscoelasticity of the monolayers. This influences: (i)the physical mechanism of collective cell migration from convective to sub-diffusion, (ii)the accumulation of residual stress, (iii)the compressive stress-induced change of monolayer cohesion, and (iv)the extent of line tension and its distribution along the edge. Most of the prior work on epithelial fingering treated migrating epithelial monolayer as viscous, polar fluids[5-7]. However, migrating epithelial collectives establish strong E-cadherin-mediated cell-cell adhesion contacts[1] and behave as viscoelastic solids[16]. Viscoelasticity, characterized by the mechanisms of energy storage and dissipation, is influenced by the cell packing density[17]. Viscoelasticity governs how stress propagates and relaxes within the monolayer, how cells redistribute mechanical stress, and how the edge responds to local perturbations. Incorporating viscoelasticity into models of epithelial fingering is therefore essential to understand fully the physical principles controlling edge stability, finger initiation, and subsequent supracellular responses.

Trenado et al.[7] highlighted the role of frictional effects on epithelial fingering. Dynamical friction has been related to the remodelling of cell-matrix adhesion contacts, while the wear along the substrate is often disregarded[18]. However, the strength of cell-matrix adhesion contacts relative to cell-cell adhesion contacts influences the epithelial spreading factor, which in turn induces epithelial wetting (extension) and de-wetting (compression) via collective cell migration and thermodynamic mixing effects between the monolayer and substrate[19]. Alert et al.[6] emphasized the role of epithelial surface tension and cell traction in epithelial fingering. The epithelial surface tension was treated as a constant[6]. Nevertheless, the epithelial surface tension, which serves as an indicator of epithelial cohesiveness, is dependent on both space and time due to the effects of dilational viscoelasticity[20].

The interplay between: (i)spreading factor, (ii)line tension gradient, (iii)distribution of residual stress, (iv)distribution of cell-matrix adhesion contacts, and (v)cell tractions determines whether local perturbations are damped, leading to a smooth edge, or amplified, resulting in finger formation. By elucidating how these parameters interact, we can connect classical concepts from soft-matter physics, such as elastic instabilities with Marangoni-like flows, to the complex, active mechanics of living epithelial tissues, providing a framework within which to understand both the physiological and pathological behaviors of epithelial monolayers.

2. Epithelial wetting/de-wetting on substrate matrices and fingering along the edge

Morphogenesis, tissue regeneration, and cancer invasion encompass dynamic changes in tissue morphology, and they occur via collective cell migration. These changes can be interpreted as the active and passive wetting and de-wetting processes of epithelial monolayers[19]. Similar to other soft-matter systems, monolayers experience extension (wetting) or compression (de-wetting) on substrates, contingent upon the equilibrium of cohesion properties within an epithelial monolayer and cell-matrix adhesion[16,19-22]. The potential of a monolayer to wet or de-wet depends on the sign and magnitude

of the spreading factor, which was discussed in the literature [16,19-22]. This factor can be expressed as: $S^e = e_a - e_c$ (where e_a is the cell-matrix adhesion energy per unit area equal to $e_a = \rho_a \frac{1}{2} k \Delta \vec{r}_B^{\,2}$, ρ_a is the surface number density of cell-matrix adhesion contacts, k is the spring constant of the single bond, $\Delta \vec{\boldsymbol{r}}_{\boldsymbol{B}}$ is the bond extension equal to $\Delta \vec{\boldsymbol{r}}_{\boldsymbol{B}} = \vec{\boldsymbol{u}}_{\boldsymbol{c}} - \vec{\boldsymbol{u}}_{\boldsymbol{s}}$, $\vec{\boldsymbol{u}}_{\boldsymbol{c}}$ is the monolayer displacement field, $\vec{\boldsymbol{u}}_{\boldsymbol{s}}$ is the substrate displacement field, e_c is the cell-cell cohesion energy per unit area (i.e., the energy required to separate a multicellular system into two parts by creating two homotypic multicellular surfaces) which is $e_c = 2\gamma_e$, and γ_e is the epithelial surface tension in contact with liquid medium. When the spreading factor is $S^e > 0$, epithelial monolayers undergo wetting, while in the case of $S^e < 0$, the monolayers undergo de-wetting[16].

Unlike passive materials, multicellular systems actively modulate specific cohesion and adhesion energies through actomyosin contractility and the remodelling of adhesion contacts. Consequently, an epithelial monolayer undergoes oscillatory wetting/de-wetting. Extension (wetting) of the monolayer caused by collective cell migration induces an increase in cohesive energy relative to adhesion energy which triggers de-wetting. De-wetting (compression) stimulates cell-cell interactions causing a decrease in cohesion energy relative to adhesion energy and the monolayer undergoes wetting again. Passive mechanical effects, such as Poisson's effect, also contribute, particularly in anisotropic regions[23]. The average Poisson's ratio of MDCK and HeLa epithelial monolayers is $\nu \sim 0.77$[24]. When the Poisson's ratio $\nu > 0.5$, extension in the *x*-direction induces compression in the *y*-direction and *vice versa*. It means that: (i)wetting can be characterised by $\varepsilon_{xx} > 0$ and $\varepsilon_{yy} < 0$ and (ii)de-wetting can be characterised by $\varepsilon_{xx} < 0$ and $\varepsilon_{yy} > 0$ (where ε_{xx} and ε_{yy} are the normal strain components).

The experimental studies conducted by Serra-Picamal et al.[25], Notbohm et al.[26], Tlili et al.[27], and Pérez-González et al.[20] have validated the inhomogeneous distributions of cell packing density, cell velocity, distributions of adhesion strength, cell tractions, and stress-strain. Notbohm et al.[26] also explored the anisotropic characteristics of mechanical stress in cells due to collective migration. Furthermore, Pérez-González et al.[19] have quantified the inhomogeneous distribution of cell-cell adhesion strength, which contributes to the inhomogeneous distribution of epithelial cohesion energy. Serra-Picamal et al.[25] highlighted that there is significant cell traction at the edge of the monolayer, whereas the traction exerted by cells in the central area of the monolayer is nearly negligible. While epithelial MDCK cell monolayers undergo wetting, some domains near the edge undergo de-wetting even after only 2 h[25] as shown schematically in **Figure 1**:

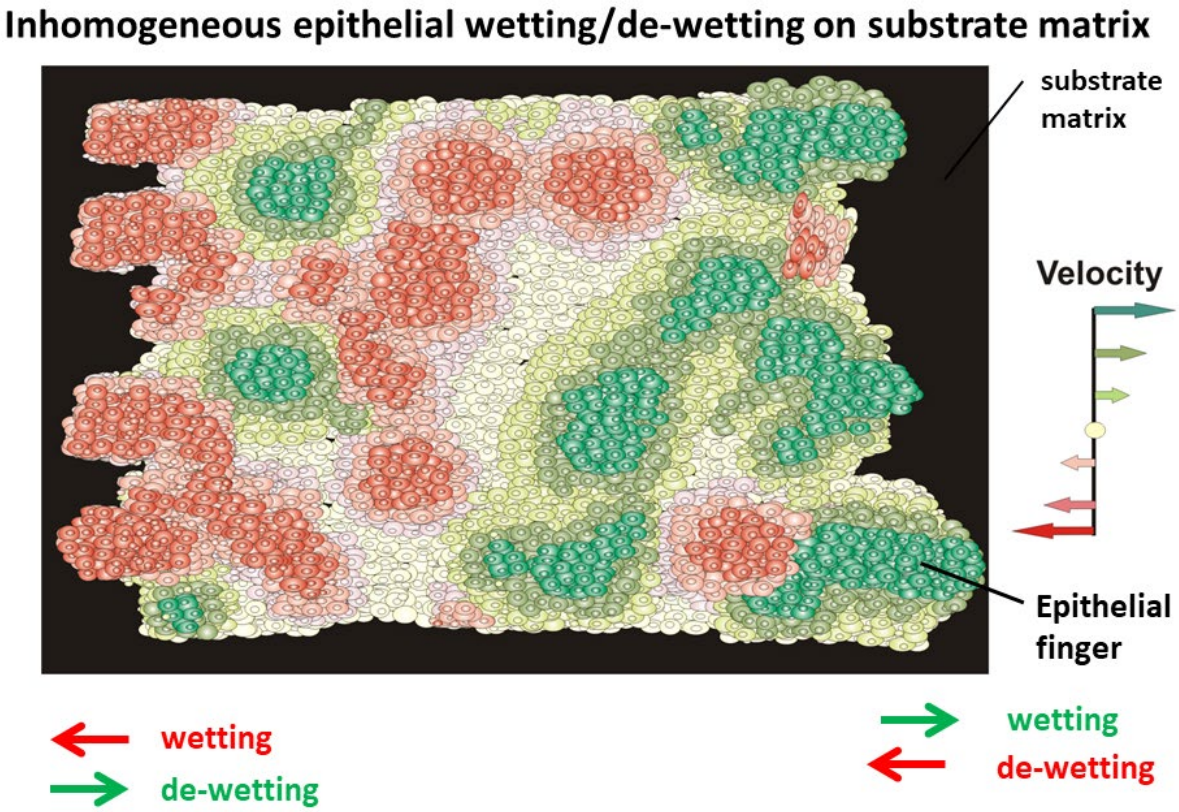

Figure 1. Inhomogeneous wetting/de-wetting of an epithelial monolayer inspired by experimental data from Serra-Picamal et al. [25]. It possesses a distribution of multicellular domains characterized by their cell velocity, packing density, stress, strain, and spreading factor.

These spatial variations lead to the formation of domains with approximately uniform physical properties, which are inherently unstable and interact with neighbouring domains, generating local forward and backward flows. Each domain has two degrees of freedom: spatial deformation and translational displacement of its center of mass. Domains can undergo uni-axial or biaxial extension/compression. Isotropic domains deform equally in all directions, driven predominantly by active process such as collective cell migration. In contrast to isotropic domains, anisotropic domains undergo uni-axial deformation by combining active and passive processes. The active process takes place through collective cell migration along the deformation axis, whereas the passive process occurs perpendicular in the migration direction due to Poisson's effect. Two possible outcomes can occur at the monolayer edge during epithelial wetting/de-wetting: (i)fingering or (ii)a smooth edge, depending on the magnitude and spatial distribution of the line tension along the edge, as shown in **Figure 2**:

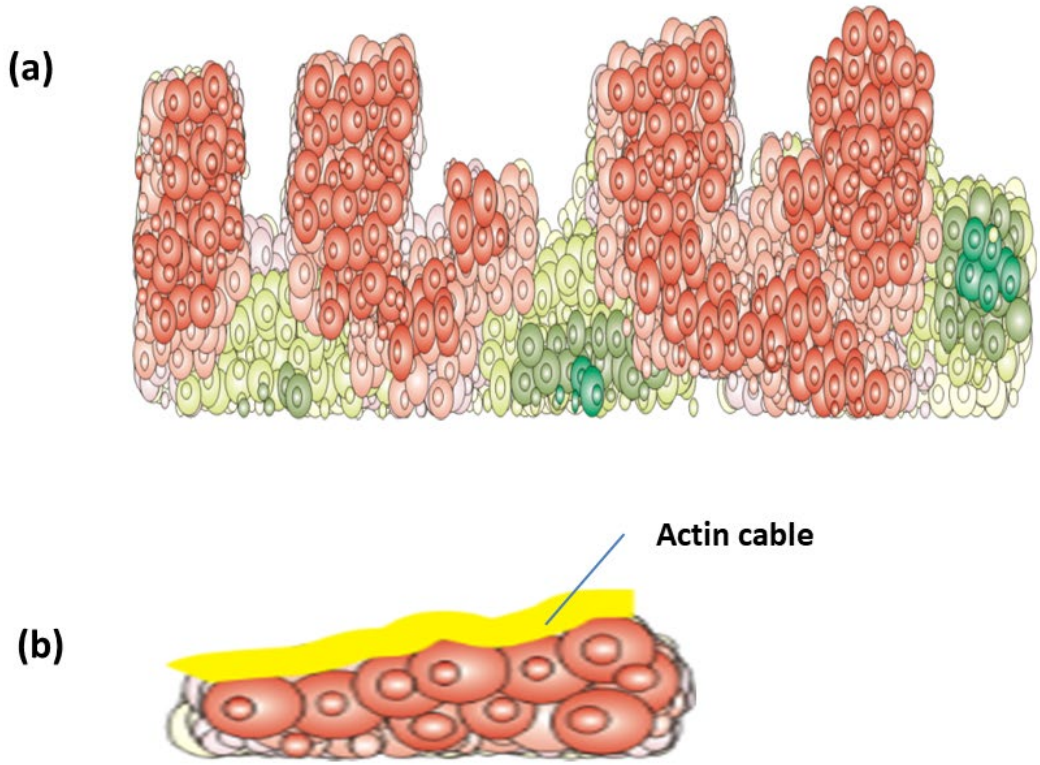

Figure 2. (a) Fingering instability at the epithelial monolayer edge without actin cable and (b) smooth-edge morphology at the monolayer boundary caused by presence of actin cable during wetting/de-wetting. The presence of a supracellular actin cable can stabilize the edge and against fingering.

Collisions between domains experiencing forward flow and adjacent domains undergoing backward flow result in the generation of compressive stress, which in turn leads to an increase in cell packing density, at the edge[17,25]. An increase in cell packing density enhances interactions between cells, resulting in a transition from anisotropic to isotropic cell migration and a reduction in cell velocity. Certain domains at the periphery migrate more rapidly than adjacent domains, resulting in the disruption of some cell-cell adhesion contacts along the edge, which subsequently induces epithelial fingering. The localized disruption of cell-cell adhesion contacts promotes the development of leader cells in specific cell types by facilitating fingering.

We have introduced a new interpretation of epithelial fingering based on effective line tension along the free edge. Although line tension is a classical mechanical concept, its use to describe fingering instabilities in migrating epithelial monolayers is, to our knowledge, novel. Energy dissipation per unit length caused by the remodelling of the edge $\lambda_d(s,\tau)$ depends on the relationship between the input of spreading energy per line and the resistance of the edge expressed in the form of line tension. The cell

spreading energy per unit length depends on the spreading factor and can be expressed as: $\frac{dE_{spread}}{ds} = S^e l_c$ (wherel_c is the average size of single cell). The line tension $\lambda(s,\tau)$ represents the storage of elastic and contractile energy per unit length. Consequently, the energy dissipation per unit length can be expressed as: $\lambda_d(s,\tau) = \frac{dE_{spread}}{ds} - \Delta\lambda$ (where$\Delta\lambda$ is the increment of storage energy per edge). The magnitude of the line tension, as well as its distribution along the edge, plays a crucial role in determining the fingering. Additionally, it is vital to define line tension as a fundamental physical parameter that greatly affects the epithelial fingering.

3. Line tension along the edge of epithelial monolayers

The edge of the monolayer consists of interconnected border cells. The line tension of the edge represents the free energy per unit length[28]. In the context of the epithelial monolayer edge, the free energy encompasses multiple contributions, including: (i)the elastic and contractile energies of border cells, (ii)the cohesion energy, and (iii) the elastic and bending energies associated with the supracellular actin cable. Consequently, total line tension can be expressed as:

$$\lambda(s,\tau) = \lambda_{cable} + \lambda_{cell} \quad (1)$$

where τ is the time of hours, which corresponds to collective cell migration, s is the coordinate along the edge, λ is the total line tension along the monolayer edge, and λ_{cell} is the contribution of the border cells, while λ_{cable} is the contribution of the actin cable to the edge line tension.

3.1 Contribution of border cells to the supracellular line tension

The contribution of border cells to the supracellular line tension depends on the epithelial surface tension and can be expressed as:

$$\lambda_{cell}(s,\tau) = \gamma_e l_c \quad (2)$$

where γ_e is the dynamic epithelial surface tension $\gamma_e = \frac{\partial E_{cells}}{\partial A}$, $dA = ds l_c$ is the surface area of border cells, $E_{cell} = \sum_i \frac{K}{2}(A_{ci} - A_0)^2 + \sum_{i,j} \Lambda l_{ij} + \sum_i \frac{T_{con\,i}}{2} {L_i}^2$, A_{ci} is the effective surface area of the i-th cell, K is an effective modulus of the cell around its initial surface area A_0, l_{ij} is the interface length between the i-th and j-th cells, Λ is the line tension per unit interface length between two cells $\Lambda = \frac{\langle N_{AJ} e_A^{AJ} \rangle}{\langle l \rangle}$, N_{AJ} is the number of adherens junctions within the interface between two neighbor cells located at the aggregate surface, e_A^{AJ} is the energy per single adherens junction, $\langle l \rangle$ is the averaged interface length between two adjacent cells, $T_{con\,i}$ is the contractility coefficient, and L_i is the perimeter of the i-th cell[29].

The dynamic epithelial surface tension γ_e is a space-time-dependent physical parameter, which is influenced by a variety of factors, including the contractility of cells, the adhesive strength of homotypic cell-cell interactions, and the deformation of multicellular surfaces, which can manifest as either stretching or compression[20,30,31]. The contractility exhibited by epithelial cells serves to strengthen the adhesion contacts between cells, thereby contributing to an increase in the epithelial surface tension[30]. Stretching and compression of monolayers have the opposite effect. While stretching leads to an increase in epithelial surface tension[31], compression enhances cell-cell interactions, resulting in a reduction of the surface tension[20].

Although the surface tension of multicellular systems is expected to exhibit spatiotemporal variations due to the viscoelasticity of multicellular surfaces and active cellular processes, direct experimental measurements have thus far accessed only static (equilibrium) values. These static surface tensions have been measured using several experimental approaches, including uniaxial compression of multicellular spheroids between parallel plates[32], micropipette aspiration[31], and magnetic tensiometry[33]. Reported surface tension values are in the range of a few $\frac{mN}{m}$ to several tens of $\frac{mN}{m}$ depending on both, cell type and the measurement technique employed[32-34]. In particular, the application of magnetic fields has been shown to strengthen cell–cell adhesion contacts, leading to an increase in the measured surface tension[35].

The line tension contribution λ_{cell} can be estimated from experimental values of static epithelial surface tension. It is equal to $\lambda_{cell} \sim 1-10$ nN, for the average cell size of $l_c \sim 10$ μm. However, the line tension is not constant. It varies along the edge depending on the state of the border cells and the strength of cell-cell adhesion contacts.

The change in the line tension contribution λ_{cell} can be formulated by establishment of the constitutive model for epithelial surface tension $\Delta\gamma_e$ vs. $\frac{\Delta A}{A}$. In alignment with the principles of dilational viscoelasticity observed in multicellular surfaces, the alteration in surface area $\frac{\Delta A}{A}$ results in energy storage and dissipation, which subsequently causes a variation in surface tension $\Delta\gamma_e$. The epithelial surface tension contributes to a reduction in the multicellular surface $\frac{\Delta A}{A}$ during: (i)the compaction of epithelial spheroids[30], (ii)the rounding of cell aggregates after uni-axial compression[32,36], (iii)the de-wetting of cell aggregates on rigid substrates[22], and (iv)the fusion of epithelial aggregates[16]. An increase in the rate of change of cell aggregate surface area $\frac{d}{d\tau}\left(\frac{\Delta A}{A}\right)$ induces an increase in the surface tension[31].

A constitutive model accounting for all of these conditions was expressed as[20]:

$$\Delta\gamma_e = E_S\frac{\Delta A}{A} + \eta_S\frac{d}{d\tau}\left(\frac{\Delta A}{A}\right) \quad (3)$$

where E_S is the surface modulus of elasticity, and η_S is the surface viscosity.

In further consideration, it is necessary to estimate the contribution of actin cable to the line tension along the edge.

3.2 Viscoelasticity and line tension of actin cable

An actin cable consists of interconnected segments, each formed by bundles of actin filaments cross-linked by actin-binding proteins inside the cells. The cable's mechanical properties emerge from the mechanics of these segments and their connections, so that each segment behaves as a polymer-like unit capable of stretching, bending, and transmitting forces. Crosslinking proteins maintain connectivity through dynamic, reversible interactions, analogous to bonds in a polymer chain. In epithelial monolayers, actin cables can span multiple cells across adherens junctions, enabling stress transmission along the tissue edge. Such supracellular actin cables form preferentially along tissue edges, where broken force balance and anisotropic tension align actomyosin contractility parallel to the boundary, stabilizing stress transmission across adherens junctions. During inhomogeneous epithelial wetting or de-wetting, the edge-localized actin cable undergoes local bending and stretching or compression in response to perpendicular forces. Stretching/compression of individual bundle of actin filaments have been described by the Kelvin-Voigt model[37]. Consequently, total line tension of actin cable includes strain energy, bending energy, and contractile energy contributions per unit length and can be expressed as:

$$\lambda_{cable}(s,\tau) = \lambda_{bend}^{cable} + \lambda_{el}^{cable} + \lambda_{cont}^{cable} \quad (4)$$

where λ_{bend}^{cable} is the bending contribution to the line tension of the cable equal to: $\lambda_{bend}^{cable} = \frac{\kappa}{2}\left(\frac{d\theta}{ds}\right)^2$, $\theta(s)$ is the angle between the tangent to the edge and the direction of cell migration, κ is the bending modulus, λ_{el}^{cable} is the elastic contribution equal to: $\lambda_{el}^{cable} = \frac{E_{AC}}{2}\varepsilon_{AC}^2 r_c^2 \pi$, E_{AC} is the Young's modulus, ε_{AC} is the local strain of the cable, r_c is the radius of the cable equal to $0.5 - 1$ μm[38], λ_{cont}^{cable} is the contractile contribution of the cable. The elastic modulus of contractile epithelial MDCK monolayers is approximately $E_c \sim 33$ kPa[39]. Although a direct Young's modulus of the supracellular actin cable has not been measured, multiple studies demonstrate that the cable sustains higher tensile stress and stores more mechanical energy than the bulk monolayer, indicating a larger effective stiffness, i.e., $E_{AC} > E_c$[9,40,41]. More contractile cable has higher elastic modulus[42]. For the supposed elastic modulus $E_{AC} = 2E_c$ and 2% strain, $\lambda_{el}^{cable} = 0.04$ nN. The bending modulus of individual actin filaments is $7x10^{-26}$ Jm [43]. The bending modulus of actin cable (being a bundle of actin filaments) should be an order of magnitude larger than the bending modulus of an individual actin filament. For the curvature of $\sim\frac{1}{50}$ μm^{-1}, the bending contribution λ_{bend}^{cable} is $\lambda_{bend}^{cable} = 1.4x10^{-7}$ nN. Deguchi et al.[44] pointed out that the contractile contribution to line tension of actin bundles is $\lambda_{cont}^{cable} \sim 4$ nN. As a result, the contractile contribution to the line tension of an actin cable represents the largest contribution, comparable in magnitude to that of the border cells. In contrast, the contribution arising from the bending of the actin cable is minimal and can be neglected. For typical cell-scale edge curvatures (~5–20 μm wavelength), bending forces are orders of magnitude smaller than contractile tension and can safely be ignored in the linear stability analysis.

3.3 Line tension gradient along the edge

The inhomogeneous storage of elastic and contractile energy along the edge during the processes of epithelial wetting and de-wetting is essential for the establishment of a line tension gradient $\frac{\partial \lambda}{\partial s}$. Certain domains near the edge experience extension, whereas others undergo compression. The degree of this extension/compression is not uniform along the line. Moderate extension of the monolayer promotes the reinforcement of cell-cell adhesion contacts[45]. Conversely, compression enhances cell-cell interactions, which leads to contact inhibition of locomotion. This contact inhibition subsequently initiates cell repolarization, which is associated with a reduction in both cell-cell and cell-matrix adhesion contacts[46]. As a result, the strength of AJs is greater in the extended regions of the edge compared to the compressed regions. Cells that are extended exhibit higher contractility than those that are compressed[47]. It is well-established that cells within stretched monolayers create a larger area of contact with the matrix[48]. Cells with greater contact area exhibit higher contractility compared to those with a smaller contact area[47]. As a result, cells located in the extended regions of edge store more elastic and contractile energy than their compressed counterparts. The supracellular actin cable functions as a semi-flexible filament[49]. Stretched semi-flexible filaments generate greater force than compressed ones when subjected to the same absolute deformation[50]. This phenomenon is associated with a nonlinear variation in force during the higher stretching or compression of individual semi-flexible filaments, as described by a worm-like chain model[51]. Stretching of actin cable can recruit additional actin and myosin along the cable, increasing its contractility and the contractile contribution to the line tension λ_{cont}^{cable}[52].

The gradient of line tension $\frac{\partial \lambda}{\partial s}$ drives cell movement along the edge from the regions of lower line tension to the regions of higher line tension as shown in **Figure 3**:

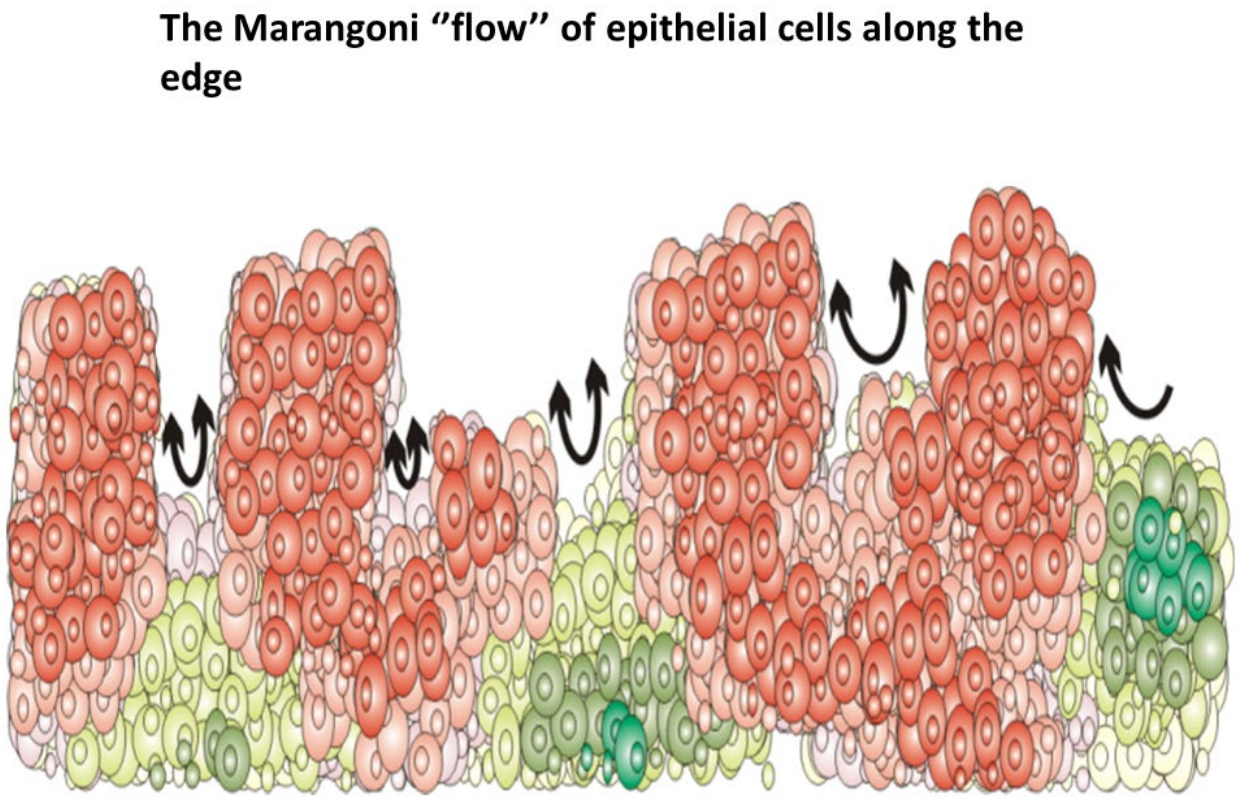

Figure 3. Migration of epithelial cells along the edge driven by the gradient of line tension (the1D Marangoni effect). Black arrows show directions of cell migration along the edge from the regions of lower line tension (gap regions) to the regions of higher line tension (finger regions).

Stretched, finger-like regions are a product of wetting, while gap-like regions are less stretched or even compressed. Higher-stretched finger-like regions of the edge have higher line tension than less stretched or compressed gap-like regions. Consequently, cells within the gaps undergo migration towards the fingers by stimulating fingering of the monolayer. The phenomenon can be discussed in the context of the 1D Marangoni effect (**Figure 2**). In general case, the Marangoni effect represents 2D migration/flow of the system constituents driven by the gradient of surface tension[53]. The Marangoni effect also influences migration of cells from the region of lower surface tension to the regions of higher surface tension[16]. While the gradient of line tension stimulates fingering of the monolayer, the line tension itself reduces fingering.

Formation of supracellular actin cable leads to: (i)an increase in the line tension and (ii)reduction of the line tension gradient. The phenomenon of epithelial fingering will be discussed based on postulated force balance along the edge.

4. Force balance along the edge

Collective cell migration in epithelial monolayers gives rise to hour-scale oscillations in velocity, strain, and accumulated residual stress[25-26]. This dynamics has been interpreted as mechanical waves and discussed in the context of low-Reynolds-number turbulence, a phenomenon also observed in viscoelastic fluids such as polymer solutions[54,55]. In migrating monolayers, this behavior has been described as active turbulence, reflecting the role of tissue viscoelasticity[56]. Mechanical waves are further linked to oscillatory wetting and de-wetting at tissue interfaces[16,19,57]. Overall, low-Reynolds-number turbulence in epithelial monolayers arises from viscoelastic effects that repeatedly perturb the dynamical balance between driving and resistive forces, leading to long-term inertial effects[16,26,57]. In the case of active turbulence in migrating epithelial collectives, the Reynolds and Weissenberg dimensionless numbers are low, i.e., R_e, $W_i \ll 1$. This effective long-term inertia emerges from two coupled processes: the accumulation of residual stresses within multicellular systems caused by collective cell migration, and cellular adaptation through: (i) the collective remodelling of cell-cell and cell-matrix adhesion contacts, (ii) cell realignment caused by glancing interactions, and (iii) repolarisation caused by cell head-on interactions [16]. Consequently, long-time inertia accounts for delayed cellular adaptation, which occurs over hours.

The force balance along the edge can be expressed as:

$$\langle m_{eff} \rangle \rho_e \frac{d\vec{\boldsymbol{v}}_{\boldsymbol{e}}(s,\tau)}{d\tau} = \sum_i \vec{\boldsymbol{F}}_{\boldsymbol{di}} - \sum_j \vec{\boldsymbol{F}}_{\boldsymbol{rj}} \quad (5)$$

where $\langle m_{eff} \rangle$ is the effective cell mass, which represents a biological inductance, ρ_e is the number density of border cells per line, $\vec{\boldsymbol{v}}_{\boldsymbol{e}}(s,\tau)$ is the epithelial velocity along the line, $\vec{\boldsymbol{F}}_{\boldsymbol{di}}$ is the i-th driving force, while $\vec{\boldsymbol{F}}_{\boldsymbol{rj}}$ is the j-th resistive force per unit line. The biological inductance results from the biological response of a single cell caused by cell-cell interactions under internally generated mechanical stress during collective cell migration. The resistive forces are: the normal component of line tension force and viscoelastic force, while the driving forces are the spreading force, mixing force, tangential component of line tension force, and traction force.

The spreading force (a driving force) $\vec{\boldsymbol{F}}_{\boldsymbol{sp}}$ is the in-plane normal force, which acts perpendicularly to the edge and can be expressed as: $\vec{\boldsymbol{F}}_{\boldsymbol{sp}}(s,\tau) = S^e \vec{\boldsymbol{n}}$ (where $\vec{\boldsymbol{n}}$ is the unit in-plane normal vector to the edge). The spreading factor acts like an effective ''active pressure'' inhomogeneously distributed along the edge, which induces inward and outward curvature depending on whether the multicellular domains near the edge undergo wetting or de-wetting.

The mixing force $\vec{\boldsymbol{F}}_{\boldsymbol{mix}}(s,\tau)$ (a driving force) is caused by thermodynamic mixing between the epithelial monolayer and substrate matrix. This is a tangential force, which correlates with the distribution of adhesion energy along the line and can be expressed as: $\vec{\boldsymbol{F}}_{\boldsymbol{mix}} = -l_c \frac{\partial}{\partial s} e_a \vec{\boldsymbol{t}}$ (where $\vec{\boldsymbol{t}}$ is the unit in-plane tangential vector to the edge). If a segment of the edge has lower cell-matrix adhesion energy, the edge pulls itself toward regions of higher adhesion energy along the edge. The phenomenon is known as *haptotaxis*[58].

The traction force $\vec{\boldsymbol{F}}_{\boldsymbol{t}}(s,\tau)$ (a driving force) pulls against the substrate (protrusion-driven migration). It depends on the viscoelasticity of the substrate matrices. The relationship between the traction force and the displacement of the substrate can be presented in the form of the Zener constitutive model[59]: $\tau_F \frac{d\vec{\boldsymbol{F}}_{\boldsymbol{t}}}{d\tau} + \vec{\boldsymbol{F}}_{\boldsymbol{t}} = E_s(s)\vec{\boldsymbol{u}}_{\boldsymbol{s}} + \eta_s(s)\frac{d\vec{\boldsymbol{u}}_{\boldsymbol{s}}}{d\tau}$ (where $\vec{\boldsymbol{u}}_{\boldsymbol{s}}$ is the displacement field, τ_F is the relaxation time of the traction force under constant displacement, $E_s(s)$ is the elastic modulus of the matrix, and $\eta_s(s)$ is the viscosity of the matrix). The traction force has tangential and normal components.

The line-tension force $\vec{\boldsymbol{F}}_{\boldsymbol{L}}(s,\tau)$ (a driving and resistive force) appears as a consequence of the inhomogeneous distribution of line tension and it can be expressed as: $\vec{\boldsymbol{F}}_{\boldsymbol{L}} = \frac{\partial}{\partial s}\left(\lambda\vec{\boldsymbol{t}}\right)$. The tangential component of the line tension force causes migration of epithelial cells along the line from the regions of lower line tension towards the regions of higher line tension (the Marangoni flow) and is equal to $F_L^t = \frac{\partial\lambda}{\partial s}$. This force drives fingering. The normal in-plane line tension force acts to reduce curvature of the edge and is equal to: $F_L^n = \lambda\kappa$ (where κ is the curvature $\kappa = \frac{\partial\theta}{\partial s}$, and θ is the local angle of the curvature). These opposite effects of normal and tangential components of the line-tension force can be discussed based on a stability analysis. When the edge is locally perturbed to $y = \xi(x,\tau) = \xi_0 e^{\omega\tau + ikx}$ (where $\xi(x,\tau)$ is the edge local displacement, ξ_0 is the amplitude of perturbation, k is the x-component of the wave vector, and ω is the angular velocity of the perturbation), this perturbation causes: (i) the generation of a small curvature equal to: $\kappa = \frac{\partial^2\xi}{\partial x^2} = -k^2\xi$ and (ii) a change in the line tension from $\lambda = \lambda_0$ to $\lambda = \lambda_0 + \delta\lambda$ (where the small perturbation of the line tension is supposed to be proportional to the perturbation $\xi(x,\tau)$, i.e., $\delta\lambda = A\xi(x,\tau)$, and A is the proportionality coefficient that describes how changes in the edge displacement modulate the local line tension). For small perturbations of the edge, it can be supposed that $\frac{\partial\lambda}{\partial s} \approx \frac{d\,\delta\lambda}{dx}$. Consequently, the normal component of the line-tension force is equal to: $F_L^n = -(\lambda_0 + A\xi)k^2\xi$, while the tangential component is: $F_L^t = Ak\xi$. In accordance with fact that F_L^n is $F_L^n < 0$, this force stabilises the edge. However, F_L^t is $F_L^t > 0$ and destabilise the edge via the 1D Marangoni effect. While the 1D Marangoni effect drives epithelial fingering, the 2D Marangoni effect caused by the gradient of epithelial-matrix interfacial tension influences the wetting/de-wetting of epithelial monolayers [60]. Actin cable has the potential to (i) reinforce the edge by increasing the line tension and the normal component of the line tension force and (ii) reduce the distribution of the line tension along the edge by decreasing the tangential component of the line tension.

The viscoelastic force $\vec{\boldsymbol{F}}_{\boldsymbol{vs}}(s,\tau)$ (a resistive force) depends on the stress distribution along the monolayer during epithelial wetting/de-wetting and can be expressed as: $\vec{\boldsymbol{F}}_{\boldsymbol{vs}}(s,\tau) = l_c^2\nabla\tilde{\boldsymbol{\sigma}}$ (where $\tilde{\boldsymbol{\sigma}}(r(s,\tau),\tau)$ is the mechanical stress). This force includes tangential and normal components. The stress can be normal (tensional or compressive) or shear. While wetting induce the generation of tensional stress, compressive stress is generated during: (i) de-wetting and (ii) collision between forward and backward flow along the edge. Inhomogeneous wetting/de-wetting of various multicellular domains results in the generation of shear stress along the biointerface between neighbouring domains. While tensional stress decreases the cell packing density, compressive stress increases it. Shear stress has no impact on cell packing density, but has the potential to perturb aligned cell migration. An increase in cell packing

density causes a change in: (i)the mechanism of cell migration from convective to sub-diffusion and (ii)the state of viscoelasticity. Epithelial monolayers behave as viscoelastic solids in accordance with fact that cells establish strong cell-cell adhesion contacts and migrate as compact clusters[1,16,17]. Three regimes of viscoelasticity are presented in **Box1**:

Box1.Regimes of viscoelasticity caused by change the cell packing density

Regime1: Cell packing density $n_e \leq n_c$ (where n_c is the cell packing density under confluent state). Petitjean et al. [61] demonstrated that the MDCK cell monolayers attained confluence at a cell packing density of $n_{conf} \sim 2.5x10^5 \ \frac{\text{cells}}{\text{cm}^2}$.
Cell migration occurs via a convective mechanism. The velocity correlation length is an order of magnitude higher than the size of single cells[62]. This means that cells perform directional migration characterised by a higher degree of anisotropy. Consequently, cells undergo uni-axial extension/compression in this regime. While active extension/compression occurs in the direction of cell migration, passive compression/extension occurs perpendicularly to this direction via Poisson's effect[23]. The viscoelasticity caused by collective cell migration can be characterised by the Zener constitutive model. The main characteristics of the Zener model is that: (i)stress can relax under constant strain conditions, and (ii)strain can relax under constant stress conditions. The stress relaxation time is a few minutes, while the strain relaxation time is a few hours[16,36,48]). The energy dissipation in this regime is primarily caused by the remodelling of cell-cell and cell-matrix adhesion contacts, which occurs over minutes[17].
Regime2: Cell packing density $n_c < n_e < n_j$ (where n_j is the cell packing density in the jamming state, which is an order of magnitude higher than n_c)
Cell migration occurs via a diffusion (conductive) mechanism. The cell speed is much lower than that in the convective regime. Intensive cell-cell interactions caused by an increase in cell packing density perturb aligned cell migration. The velocity correlation length decreases. Consequently, this regime corresponds to isotropic cell migration such that active extension/compression occurs equally in all directions. Stress relaxation is supressed. The energy dissipation in this regime is primarily caused by perturbation of cell alignment, which occurs over hours. In accordance with the fact that diffusion is a linear process, the corresponding constitutive model of viscoelasticity should be also linear. The Kelvin-Voigt model was proposed for describing the viscoelasticity in this regime[16].
Regime3: Cell packing density $n_e \rightarrow n_j$
This regime corresponds to the state of a multicellular system near jamming. Cell migration occurs via a non-linear, sub-diffusion mechanism. The non-linearity is caused by damping of the cell rearrangement caused by an increase in cell packing density, which has been described by fractional derivatives. The perturbation of cell alignment in this regime induces anomalous energy dissipation, which occurs over hours[17]. The cell speed tends to zero. The velocity correlation length corresponds to the size of single cell[60]. Pajic-Lijakovic et al.[16] proposed the fractional model to describe viscoelasticity of cell monolayers in this regime.
An increase in the frequency of cell head-on interactions from regime 2 to regime 3 intensifies the contact inhibition of locomotion, which represents the main cause of the cell jamming state transition[16]. The contact-inhibition of locomotion triggers cell repolarisation and migration in the opposite direction[46]. The jamming state transition is the contractile-to-non contractile cell state transition[16]. When the time between two collisions becomes shorter than the cell re-polarisation time, cells cannot establish their active, migratory state again and undergo jamming.

The existence of these distinct viscoelastic regimes points to a physical mechanism of cell migration that is closely connected to the viscoelasticity of the cell monolayer and consequently helps to illuminate the mechanism(s) of energy storage and dissipation. Energy storage within the edge is a prerequisite of edge stabilization and has the potential to protect epithelial fingering.

When the spreading factor is $S^e > 0$, epithelial cells undergo inhomogeneous wetting. The wetting causes: (i)inhomogeneous accumulation of tensional stress within the monolayer and along the edge by increasing the viscoelastic force and (ii)inhomogeneous extension of the edge by increasing the normal component of the line tension force. Both forces, i.e., the normal component of the line tension force and viscoelastic force act to reduce further extension of the monolayer, leading to decrease of the cell velocity. A decrease in cell velocity causes a decrease in the traction force. Extension of the monolayer

reinforces the strength of cell-cell adhesion contacts by increasing the epithelial cohesion energy relative to cell-matrix adhesion energy. This increase in the strength of cell-cell adhesion contacts and epithelial surface tension leads to a decrease in the spreading factor, as well as in the spreading force. Collective cell migration during epithelial wetting tends to smooth cell-matrix adhesion gradients by decreasing the mixing force. When cohesion energy becomes higher than adhesion energy, the spreading factor is $S^e < 0$. In this case, epithelial cells undergo local de-wetting, i.e. compression. The compression of epithelial domains enhances cell-cell interactions leading to contact inhibition of locomotion. These interactions results in a decrease in strength of cell-cell adhesion contacts leading to an increase in the spreading factor and a decrease in the line tension. If the spreading factor is $S^e > 0$, cells undergo wetting again. A decrease in the line tension leads to epithelial fingering. While some epithelial domains near the edge undergo wetting, surrounding domains undergo de-wetting producing forwards and backwards flows along the edge. Collision between forward and backward flow causes an increase in cell packing density, which can lead to a change in the regime of viscoelasticity of the monolayer. In accordance with the observation that epithelial surface tension and mechanical stress oscillate during epithelial wetting/de-wetting[20,25,26], it is expected that the line tension along the edge also oscillates, despite the fact that spatiotemporal variations in line tension have not yet been experimentally measured.

For fingering to occur, several conditions should be satisfied: (i)$\lambda < \lambda_c$ (where λ_c is the critical threshold $\lambda_c \sim \lambda_{cell}$), (ii) $\frac{\partial \lambda}{\partial s} \neq 0$, and (iii)$\nabla \widetilde{\boldsymbol{\sigma}} \neq 0$. In contrast, increases in: (i) the line tension due to the presence of actin cable and (ii) cohesion energy relative to adhesion energy have the potential to reduce epithelial fingering. Consequently, some epithelial cell types do not show fingering even without actin cable, if these cells establish stronger cell-cell adhesion contacts. The presence of an actin cable can stabilise the monolayer edge by: (i) increasing the line tension and (ii) reducing the variation of line tension along the edge.

5. The relationship between physical parameters that govern epithelial fingering

The volumetric and dilational viscoelastic properties of migrating epithelial monolayers affect: (i)the accumulation of mechanical stress, (ii)epithelial surface tension, (iii)the mechanism of cell migration, and (iv)the contribution of border cells along the leading edge to the line tension. The viscoelasticity depends on the strength of cell-cell adhesion contacts and cell contractility. An inhomogeneous distribution of cell-matrix adhesion contacts relative to cell-cell adhesion contacts triggers epithelial wetting/de-wetting leading to an inhomogeneous accumulation of mechanical stress. This, in turn, has a feedback effect on the cell migration mechanism and the viscoelastic state itself. The interrelationship between physical parameters is shown in **Figure 4**:

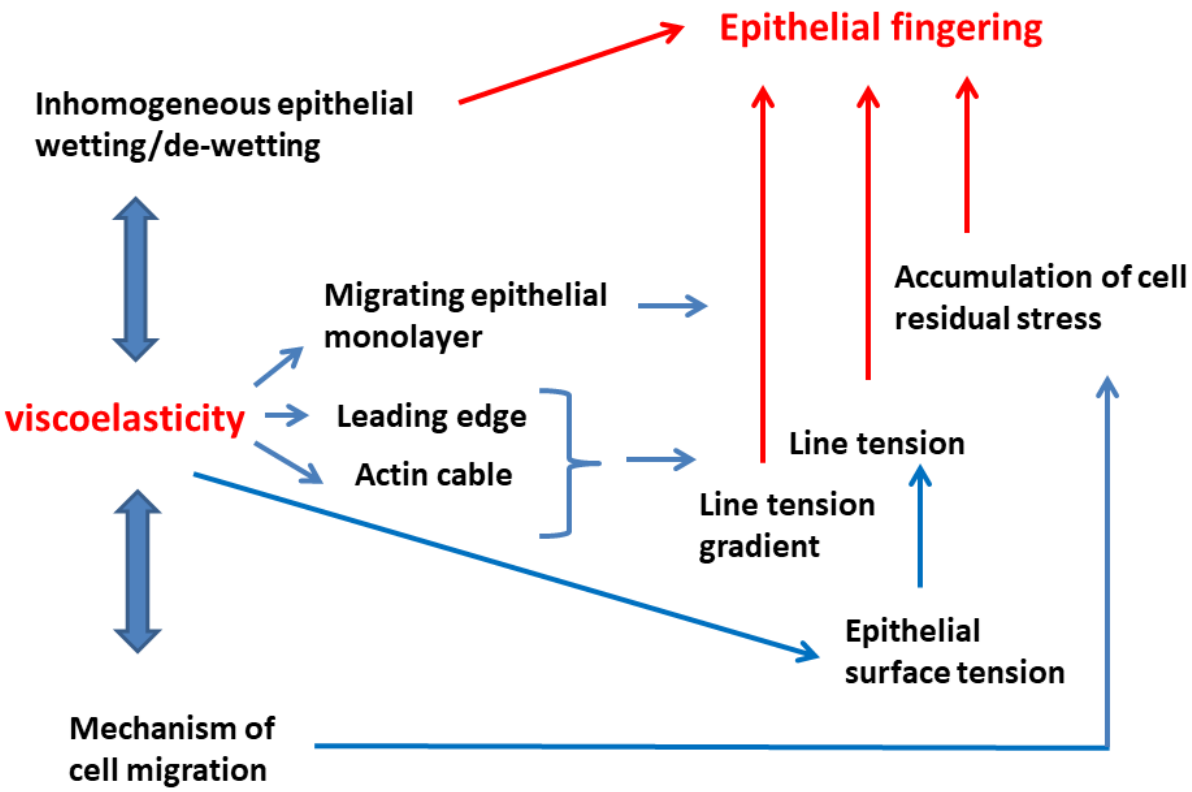

Figure 4. The inter-relationship between physical parameters responsible for epithelial fingering (The red colour emphasizes the cause-consequence relationship between viscoelasticity and epithelial fingering.)

An inhomogeneous distribution of mechanical stress and the mechanism of cell migration along the edge contribute to the formation of a line tension gradient. The interplay of these physical factors has the capacity to destabilize the edge and initiate epithelial fingering. In order to achieve a deeper comprehension of epithelial fingering, additional experiments are needed to ascertain several physical parameters, including the distributions of: (i) epithelial surface tension across the monolayer and its variations during the processes of epithelial wetting and de-wetting [63], (ii) epithelial line tension at the edge of the monolayer, (iii) epithelial-matrix adhesion energy per unit area, (iv) residual stress within cells, and (v) the density of cell packing, which correlates with cell velocity. Certain parameters have already been quantified, such as: the distribution of cell stress [25], cell packing density [27], and cell tractions [19] within the migrating epithelial monolayer. The surface density of cell tractions may be associated with the epithelial-matrix adhesion energy, represented by the equation $e_a = \int_0^{|\Delta\vec{r}_B|} T_n d(|\Delta\vec{r}_B|)$ (where T_n is the normal component of the surface density of cell tractions, which can be correlated with the normal component of the line tension force $F_{tn} = T_n l_c$). While it is established that the epithelial surface tension fluctuates with both time and spatial context (i.e., dynamic surface

tension), there is a lack of empirical evidence to substantiate the idea of temporal variations in this physical characteristic. Up to this point, only a static (equilibrium) measurement of surface tension has been recorded and identified as a feature of multicellular surfaces interacting with a liquid medium. The distribution of epithelial line tension along the edge of the monolayer and its temporal changes remain unmeasured.

Given multiple effective parameters (viscoelastic moduli, line tension, adhesion, and cohesion energy per unit surface, cell residual stress discussed within three cell packing density regimes), the uncertainty should be assessed. Bayesian inference provides a practical framework, combining prior knowledge with experimental data to yield posterior distributions, credible intervals, and parameter correlations, ensuring robust and interpretable model predictions [64].

6. Outlook: experimental tests

Experimental validation of theoretically predicted mechanical instabilities, including fingering, in epithelial monolayers can be achieved using contactless or minimally invasive approaches that probe intrinsic surface and line tensions, as well as cell mechanical stress. The estimated ranges of these physical parameters and proposed measuring techniques are shown in **Table 1**:

Table 1. Physical parameters: ranges and proposed experimental techniques

Physical parameter	The range of the parameter	Experimental technique
Line tension λ	A few nN to a few tens of nN	laser ablation
Epithelial surface tension γ_e	A few $\frac{\mathrm{mN}}{\mathrm{m}}$ to a few tens of $\frac{\mathrm{mN}}{\mathrm{m}}$	embedded elastic microbead sensors and imaging of monolayer curvature
Cell mechanical stress $\tilde{\boldsymbol{\sigma}}$	$\leq$ a few hundred of Pa	monolayer stress microscopy
Surface density of cell tractions $\vec{T}$	$\leq$ a few hundred of Pa	traction force microscopy

Laser ablation of cell–cell junctions or supracellular actin cables combined with the 1D Kelvin-Voigt model could be used for the measurements of line tension along edges through recoil dynamics [65], while embedded elastic microbead sensors [66] quantify local isotropic compressive stress within the monolayer. High-resolution imaging of monolayer geometry and curvature, combined with these measurements, allows reconstruction of intrinsic epithelial surface tension near the edge based on the Young-Laplace equation. Traction force microscopy can complement these approaches by mapping the distribution of traction forces exerted on the substrate and estimating cell–matrix adhesion energy per unit area [67]. To estimate the internally generated mechanical stress within an epithelial monolayer during collective cell migration, monolayer stress microscopy has been employed [67]. Nonetheless, a limitation of this technique is the assumption that the tissue possesses linear, uniform, and isotropic

elasticity, as well as a consistent thickness [68]. Time-lapse imaging enables tracking of dynamic changes; and perturbations of actomyosin contractility or adhesion allow separation of elastic, contractile, and adhesion-mediated contributions. Together, these techniques provide a spatiotemporally resolved, quantitative map of epithelial mechanical parameters, enabling rigorous comparison with theoretical predictions of instability onset, finger formation, and propagation.

7. Conclusion

In summary, epithelial fingering emerges as a robust consequence of mechanical and adhesive heterogeneities that develop during collective cell migration. We have shown that spatial variations in mechanical stress, cell–matrix adhesion strength, cell–cell cohesion, and line-tension along the free edge provide the essential cues that break symmetry and promote the emergence of protruding domains. These inhomogeneities originate from the interplay between epithelial wetting and local de-wetting, which dynamically redistribute stresses and adhesion contacts across the monolayer. Crucially, our analysis highlights that viscoelasticity—although widely acknowledged as a dominant physical characteristic of epithelial tissues—has been largely neglected in existing fingering models, despite its central role in governing residual stress accumulation, and spatio-temporal modulation of line tension at the edge.

The gradient of line tension and the differences in cell-matrix adhesion compared to cell-cell cohesion are responsible for driving epithelial fingering. However, the distribution of residual stress and the coupling between line tension and edge curvature serve to inhibit this fingering. Consequently, line tension can play opposing roles—promoting or inhibiting finger formation—depending on its magnitude and spatial distribution along the monolayer edge. Altogether, our work proposes that epithelial fingering is not controlled by a single dominant factor but by the dynamic coupling between (i) wetting/de-wetting, (ii) residual stress accumulation, (iii) the distribution of line tension, and (iv) spatial variations in adhesion and traction forces.

Our findings provide an integrated biological and physical framework for understanding how epithelial tissues regulate the balance between stable sheet migration and protrusive instability. Future work combining live imaging, mechanical perturbations, and molecular manipulation of adhesion and cytoskeletal regulators will be essential for determining how tissues actively prevent fingering during normal development and repair, and why this control can fail in pathological contexts such as cancer invasion.

Acknowledgement This work was supported in part by the Engineering and Physical Sciences Research Council, United Kingdom (grant number EP/X004597/1) and by the Ministry of Science, Technological Development and Innovation of the Republic of Serbia (Contract No. 451-03-34/2026-03/ 200135).

Competing Interests

The authors declare no competing interests.

The list of symbols

Cell mechanical stress	$\tilde{\boldsymbol{\sigma}}$	(Pa)
Epithelial cohesion energy per unit surface	e_c	$\left(\frac{\mathrm{J}}{\mathrm{m}^2}\right)$
Epithelial-matrix adhesion energy per unit surface	e_a	$\left(\frac{\mathrm{J}}{\mathrm{m}^2}\right)$
Epithelial surface tension	γ_e	$\left(\frac{\mathrm{J}}{\mathrm{m}^2}\right) \equiv \left(\frac{\mathrm{N}}{\mathrm{m}}\right)$
Epithelial line tension	λ	(N)
Spreading factor	S^e	$\left(\frac{\mathrm{J}}{\mathrm{m}^2}\right)$

References

1. Barriga EH, Mayor R. Adjustable viscoelasticity allows for efficient collective cell migration. Sem. Cell Dev. Biol. 2019;93:55-68,doi.org/10.1016/j.semcdb.2018.05.027.
2. Shellard A, Mayor R. All roads lead to directional cell migration. Trends Cell Biol. 2020;30(11):852-868,doi.org/10.1016/j.tcb.2020.08.002.
3. Mayor R, Etienne-Manneville S. The front and rear of collective cell migration. Nature Reviews Molecular Cell Biology, 2016;17(2):97–109, https://doi.org/10.1038/nrm.2015.14.
4. Trepat X, Sahai E. Mesoscale physical principles of collective cell organization. Nature Phys. 2018;14(7),:671–682,https://doi.org/10.1038/s41567-018-0194-9.
5. Blanch-Mercader, C, Vincent R, Bazellières E, Serra-Picamal X, Trepat X, Casademunt J. Effective viscosity and dynamics of spreading epithelia: a solvable model. Soft Matter, 2017;13(6):1235–1243,https://doi.org/10.1039/C6SM02188C.
6. Alert R, Blanch-Mercader C, Casademunt J. Active fingering instability in tissue spreading. Phys. Rev. Let. 2019;122(8):088104,https://doi.org/10.1103/PhysRevLett.122.088104
7. Trenado C, Bonilla LL, Martínez-Calvo A. Fingering instability in spreading epithelial monolayers: roles of cell polarisation, substrate friction and contractile stresses. Soft Matter, 2021;17(36):8276–8290,https://doi.org/10.1039/D1SM00626F.
8. Reffay M, Parrini MC, Cochet-Escartin O, Ladoux B, Buguin A, Cáceres J, Yamao M, Dahan M, Voituriez R, Silberzan P. Interplay of RhoA and mechanical forces in collective cell migration driven by leader cells. Nature Cell Biol. 2014;16(3):217–223,DOI:10.1038/ncb2917.
9. Ravasio A, Cheddadi I, Chen T, Pereira T, Ong HT, Bertocchi C. Brézin C, Badel M, Mege RM, Lim CT, Gov NS, Ladoux B. Mechanical forces drive cell monolayer expansion. Nature Comm. 2015;6:7683,doi 10.1038/ncomms8683.
10. Vishwakarma M, Thurakkal B, Spanos CM, Dasgupta J, Balasubramaniam L, Gov NS, Rao M, Shivashankar GV. Mechanical instabilities drive collective cell migration. Nature Phys. 2020;16, 802–809,doi 10.1038/s41567-020-0875-z.
11. Yu S, Jiang H. Adhesion-Induced Instability Regulates Contact Mechanics of Soft Thin Elastic Films. ACS Applied Mat. Interf. 2021;13(18):21994–21999, https://doi.org/10.1021/acsami.1c03047.
12. Pandey M, Ahuja R, Kumar R. Viscous fingering instabilities in spontaneously formed blisters of MoS_2 multilayers. Nanoscale Adv. 2023;5(23):6617–6625,https://doi.org/10.1039/D3NA00563A
13. Yang Y, Levine H. Leader-cell-driven epithelial sheet fingering. Phys. Biol. 2020;17(4): 046003. https://doi.org/10.1088/1478-3975/ab907e.
14. Jacinto A, Woolner S, Martin P. Dynamic analysis of dorsal closure in Drosophila: A supracellular actomyosin cable. Develop. Cell, 2002;3(3):377–386,DOI: 10.1016/s1534-5807(02)00208-3.
15. Cavey M, Lecuit T. Molecular bases of cell–cell junctions stability and dynamics. Cold Spring Harbor Perspect. Biol. 2009;1(5): a002998,DOI: 10.1101/cshperspect.a002998.

16. Pajic-Lijakovic I, Milivojevic M., McClintock PVE. Epithelial cell-cell interactions in an overcrowded environment: jamming or live cell extrusion. J. Biol. Eng. 2024;18(47), DOI:10.1186/s13036-024-00442-3.
17. Pajic-Lijakovic I, Milivojevic M. Entropy Production in Epithelial Monolayers Due to Collective Cell Migration. Entropy 2025;27(5):483,DOI:10.3390/e27050483.
18. Vazquez K, Saraswathibhatla A, Notbohm J. Effect of substrate stiffness on friction in collective cell migration. Sci. Rep. 2022;12:2474,https://doi.org/10.1038/s41598-022-06504-0.
19. Pérez-González C, Alert R, Blanch-Mercader C, Gómez-González M, Kolodziej T, Bazellieres E, Casademunt J, Trepat X. Active wetting of epithelial tissues. Nature Phys. 2019; 15:79-88, DOI:10.1038/s41567-018-0279-5.
20. Pajic-Lijakovic I, Eftimie R, Milivojevic M, Bordas SPA. Multi-scale nature of the tissue surface tension: theoretical consideration on tissue model systems. Adv. Colloid Interface Sci. 2023;315:102902,DOI:10.1016/j.cis.2023.102902.
21. Douezan S, Guevorkian K, Naouar R, Dufour S, Cuvelier D, Brochard-Wyarta F Spreading dynamics and wetting transition of cellular aggregates. PNAS 2011;108(18):7315–7320, https://doi.org/10.1073/pnas.1018057108.
22. Lucia SE, Jeong H, Shin JH. Cell segregation via differential collision modes between heterotypic cell populations. Mol. Biol. Cell. 2022; 33:ar129, 1–12, DOI:10.1091/mbc.E22-03-0097.
23. Pajic-Lijakovic I, Milivojevic M, McClintock PVE. Compressibility of biological systems: the viscoelastic Poisson's ratio. Adv Phys X 2025;10(1),DOI:10.1080/23746149.2024.2440023.
24. Moisdon E, Seez P, Molino F, Marcq P, Gay C. Mapping cell cortex rheology to tissue rheology and vice versa. Phys. Rev. E 2022;106(3-1):034403,doi = {10.1103/PhysRevE.106.034403}.
25. Serra-Picamal X, Conte V, Vincent R, Anon E, Tambe DT, Bazellieres E, Butler JP, Fredberg JJ, Trepat X. Mechanical waves during tissue expansion. Nat. Phys. 2012; 8(8):628-634,DOI: 10.1038/nphys2355.
26. Notbohm J, Banerjee S, Utuje KJC, Gweon B, Jang H, Park Y, Shin J, Butler JP, Fredberg JJ, Marchetti MC. Cellular contraction and polarization drive collective cellular motion. Biophys. J. 2016;110:2729-2738,DOI:10.1016/j.bpj.2016.05.019.
27. Tlili S, Gauquelin E, Li B, Cardoso O, Ladoux B, Delanoë-Ayari H, Graner F. Collective cell migration without proliferation: density determines cell velocity and wave velocity. R. Soc. Open Sci. 2018;5:172421,doi:10.1098/rsos.172421.
28. de Gennes P-G, Brochard-Wyart F, Quéré D. Capillarity and Wetting Phenomena: Drops, Bubbles, Pearls, Waves. Springer, New York, NY,2004.
29. Koride S, Loza AJ, Sun SX. Epithelial vertex models with active biochemical regulation of contractility can explain organized collective cell motility. APL Bioeng. 2018;2:031906, DOI:10.1063/1.5023410.
30. Devanny AJ, Vancura MB, Kaufman LJ. Exploiting differential effects of actomyosin contractility to control cell sorting among breast cancer cells. Mol. Biol. Cell 2021;32:ar24, doi.org/10.1091/mbc.E21-07-0357.
31. Guevorkian K, Brochard-Wyart F, Gonzalez-Rodriguez D. Flow dynamics of 3D multicellular systems into capillaries, in Viscoelasticity and collective cell migration, eds. Pajic-Lijakovic I, Barriga E (Academic Press, US),2021;p.193.

32. Mombach JCM, Robert D, Graner F, Gillet G, Thomas GL, Idiart M, Rieu JP. Rounding of aggregates of biological cells: Experiments and simulations. Phys. A 2005;352:525-534, doi:10.1016/j.physa.2005.02.008.
33. Nagle I, Richert A, Quinteros M, Janel S, Buysschaert E, Luciani N, Debost H, Thevenet V, Wilhelm C, Prunier C, Lafont F, Padilla-Benavides T, Boissan M, Reffay M. Surface tension of model tissues during malignant transformation and epithelial–mesenchymal transition. Front. Cell Dev. Biol. 2022;DOI 10.3389/fcell.2022.926322.
34. Stirbat TV, Mgharbel A, Bodennec S, Ferri K, Mertani HC, Rieu JP, Delanoe¨-Ayari H. Fine Tuning of Tissues' Viscosity and Surface Tension through Contractility Suggests a New Role for a-Catenin. PLOS ONE 2013;8(2):e52554,DOI:10.1371/journal.pone.0052554.
35. Jafari J, Han X-I, Palmer J, Tran PA, O'Connor A.J. Remote Control in Formation of 3D Multicellular Assemblies Using Magnetic Forces. ASC Biomat. Sci. Eng. 2019;5:2532-2542, DOI:10.1021/acsbiomaterials.9b00297.
36. Marmottant P, Mgharbel A, Kafer J, Audren B, Rieu JP, Vial JC, van der Sanden B, Maree AFM, Graner F, Delanoe-Ayari H. The role of fluctuations and stress on the effective viscosity of cell aggregates. PNAS 2009;106(41):17271-17275,doi.org/10.1073/pnas.0902085106.
37. Kumar S, Maxwell IZ, Heisterkamp A, Polte TR, Lele TP, Salanga M, Mazur E, Ingber DE. Viscoelastic Retraction of Single Living Stress Fibers and Its Impact on Cell Shape, Cytoskeletal Organization, and Extracellular Matrix Mechanics. Biophy. J. 2006;90(10),:3762–3773. https://doi.org/10.1529/biophysj.105.071506.
38. Rajan S, Kudryashov DS, Reisler E. Actin Bundles Dynamics and Architecture. Biomolecules 2023;13(3):450,DOI 10.3390/biom13030450.
39. Schulze KD, Zehnder SM, Urueña JM, Bhattacharjee T, Sawyer WG, Angelini TE. Elastic modulus and hydraulic permeability of MDCK monolayers. J. Biomech. 2017; 53:210-213, DOI:10.1016/j.jbiomech.2017.01.016.
40. Hutson M.S, Tokutake Y, Chang M-S, Bloor JW, Venakides S, Kiehart DP, Edwards GS. Forces for morphogenesis investigated with laser microsurgery and quantitative modeling. Science 2003;300:145–149,https://doi.org/10.1126/science.1079552
41. Lecuit T, Lenne P-F, Munro E. Force generation, transmission, and integration during cell and tissue morphogenesis. Nature Rev. Mol. Cell Biol. 2011;12:181–190,DOI:10.1038/nrm3084.
42. Lu L, Oswald SJ, Ngu H, Yin FC-P. Mechanical Properties of Actin Stress Fibers in Living Cells. Biophys. J. 2008;95(12): 6060–6071,.doi:10.1529/biophysj.108.133462.
43. Gittes F, Mickey B, Nettleton J, Howard J. Flexural rigidity of microtubules and actin filaments measured from thermal fluctuations. J. Cell Biol. 1993;120:923–934,DOI:10.1083/jcb.120.4.923.
44. Deguchi S, Sato M, Kaibara M. Evaluation of tension in actin bundle of endothelial cells based on preexisting strain and tensile properties measurements. J. Biomech. 2005;38(11):2135-2143, DOI:10.3970/mcb.2005.002.125.
45. Acharya BR, Wu SK, Lieu ZZ, Gómez GA, Parton RG, Hamilton NA, Neufeld Z, Yap AS. A mechanosensitive RhoA pathway that protects epithelia against acute tensile stress. Develop. Cell 2018;47(4):439–452.e6,DOI: 10.1016/j.devcel.2018.09.016.
46. Roycroft A, Mayor R. Molecular basis of contact inhibition of locomotion. Cell. Mol. Life Sci. 2016;73:1119–1130,DOI:10.1007/s00018-015-2090-0.

47. Saraswathibhatla A, Notbohm J, Streichan SJ. Coordination of contractile tension and cell area changes in epithelial tissue mechanics. Phys. Rev. E, 2022;105(2),:024405, DOI:10.1103/PhysRevE.105.024404.
48. Khalilgharibi N, Fouchard J, Asadipour N, Yonis A, Harris A, Mosaff P, Fujita Y, Kabla A, Baum B, Muñoz JJ, Miodownik M, Charras G. Stress relaxation in epithelial monolayers is controlled by actomyosin. Nature Phys. 2019;15: 839-847,DOI:10.1038/s41567-019-0516-6.
49. Hannezo E, Prost J, Joanny JF. Instabilities of monolayered epithelia: Shape and structure of villi and crypts. Phys. Rev. Let. 2011;107(7): 078104, https://doi.org/10.1103/PhysRevLett.107.078104.
50. Broedersz CP, MacKintosh FC. Modeling semiflexible polymer networks. Rev. Mod. Phys. 2014;86(3):995-1036,https://doi.org/10.1103/RevModPhys.86.995.
51. Yamakawa H. Modern Theory of Polymer Solutions. Harper and Row, New York,1971.
52. Kobb AB, Zulueta-Coarasa T, Fernandez-Gonzalez R. Tension regulates myosin dynamics during Drosophila embryonic wound repair. J. Cell Sci. 2017;130(4):689–696.doi:10.1242/jcs.196139.
53. Karbalaei A, Kumar R, Cho HJ. Thermocapillarity in Microfluidics—A Review. Micromachines 2016;7:13;doi:10.3390/mi7010013.
54. Groisman A, Steinberg V. Elastic turbulence in a polymer solution flow. Nature 2000;405:53-55, DOI: 10.1038/35011019.
55. Pajic-Lijakovic I, Milivojevic M., McClintock PVE. Role of viscoelasticity in the appearance of low-Reynolds turbulence: Considerations for modelling. J. Biol. Eng. 2024;18:24, https://doi.org/10.1186/s13036-024-00415-6.
56. Alert R, Casademunt J, Joanny J-F. Active Turbulence. Annu. Rev. Condens. Matter Phys. 2022;13:143–70,https://doi.org/10.1146/annurev-conmatphys-082321-035957.
57. Deforet M, Hakim V, Yevick HG, Duclos G, Silberzan P. Emergence of collective modes and tri-dimensional structures from epithelial confinement. Nature Comm. 2014; 5:3747, https://doi.org/10.1038/ncomms4747.
58. Wen JH, Choi O, Taylor-Weiner H., Fuhrmann A, Karpiak JV, Almutairi A, Engler A J. Haptotaxis is cell type specific and limited by substrate adhesiveness. Cell. Mol. Bioeng. 2015;8(4):530–542. doi10.1007/s12195-015-0398-3.
59. Sharma V, Adebowale K, Gong Z, Chaudhuri O, Shenoy VB. Glassy Adhesion Dynamics Govern Transitions Between Sub-Diffusive and Super-Diffusive Cell Migration on Viscoelastic Substrates. bioRxiv 2025;https://doi.org/10.1101/2025.03.11.642113.
60. Pajic-Lijakovic, I., Milivojevic, M. Marangoni effect and cell spreading. Europ. Biophys. J, 2022; 51:419–429, doi.org/10.1007/s00249-022-01612-1.
61. Petitjean L, Reffay M, Grasland-Mongrain E, Poujade M, Ladoux B, Buguin A, Silberzan P. Velocity fields in a collectively migrating epithelium. Biophys. J. 2010; 98(9):1790-800, doi:10.1016/j.bpj.2010.01.030.
62. Petrolli V, Boudou T, Balland M, Cappello G. Oscillations in collective cell migration, in Viscoelasticity and Collective Cell Migration: An Interdisciplinary Perspective Across Levels of Organization, eds. by I. Pajic-Lijakovic, E. Barriga (Academic Press, US) 2021;p.157.
63. Pajic-Lijakovic I, Milivojevic M. 2023. Active wetting of epithelial tissues: modeling considerations. Europ. Biophys. J. 2023; 52:1-15, DOI:10.1007/s00249-022-01625-w.

64. Rappel H, Beex LAA, Bordas SPA. Bayesian inference to identify parameters in viscoelasticity. Mech. Time-Depend. Mater. 2017;22(2), 221–258, https://doi.org/10.1007/s11043-017-9361-0.
65. Liang X, Michael M, Gomez GA. Measurement of Mechanical Tension at Cell-cell Junctions Using Two-photon Laser Ablation. Bio-protocol 2016;6(24):e2068. DOI: 10.21767/2068
66. Dolega ME, Delarue M, Ingremeau F, Prost J, Delon A, Cappello G. Cell-like pressure sensors reveal increase of mechanical stress towards the core of multicellular spheroids under compression, Nature Comm. 2017;8:14056 1-9, DOI: 10.1038/ncomms14056.
67. Tambe DT, Croutelle U, Trepat X, Park CY, Kim JH, Millet E, Butler JP, Fredberg JJ. Monolayer Stress Microscopy: Limitations, Artifacts, and Accuracy of Recovered Intercellular Stresses. PLoS ONE 2013; 8(2):e55172 1-13, doi:10.1371/journal.pone.0055172.
68. Gómez-González M, Latorre E, Arroyo M, Trepat X. Measuring mechanical stress in living tissues. Nat. Rev. Phys. 2020; 2:300–317, doi:10.1038/s42254-020-0184-6.

Figure captions:

Figure 1. Inhomogeneous wetting/de-wetting of an epithelial monolayer inspired by experimental data from Serra-Picamal et al. [25]. It possesses a distribution of multicellular domains characterized by their cell velocity, packing density, stress, strain, and spreading factor.

Figure 2. (a) Fingering instability at the epithelial monolayer edge without actin cable and (b) smooth-edge morphology at the monolayer boundary caused by presence of actin cable during wetting/de-wetting. The presence of a supracellular actin cable can stabilize the edge and against fingering.

Figure 3. Migration of epithelial cells along the edge driven by the gradient of line tension (the1D Marangoni effect). Black arrows show directions of cell migration along the edge from the regions of lower line tension (gap regions) to the regions of higher line tension (finger regions).

Figure 4. The inter-relationship between physical parameters responsible for epithelial fingering (The red colour emphasizes the cause-consequence relationship between viscoelasticity and epithelial fingering.)

Table captions

Table 1. Physical parameters: ranges and proposed experimental techniques